Acta Crystallographica Section C
**Crystal Structure Communications**
ISSN 0108-2701

# $Al_{14}Ba_8La_{26.3}Ru_{18}Sr_{53.7}O_{167}$: a variant of cubic perovskite with isolated $RuO_6$ units

**F. J. Zúñiga,[a]* F. J. García-García,[b] M. Hoelzel[c] and A. Reller[b]**

[a]Departamento de Física de la Materia Condensada, Facultad de Ciencia y Tecnología, Universidad del País Vasco, UPV/EHU, Apartado 664, 48080 Bilbao, Spain, [b]Lehrstuhl für Festkörperchemie, Institut für Physik, Universität Augsburg, Universitätsstrasse 1, Augsburg, Germany, and [c]Fachbereich Material- und Geowissenschaften, Technische Universität Darmstadt, Petersenstrasse 23, 64287 Darmstadt, Germany
Correspondence e-mail: javier.zuniga@ehu.es

Received 10 February 2010
Accepted 14 April 2010
Online 22 April 2010

The crystal structure of the title aluminium barium lanthanum ruthenium strontium oxide has been solved and refined using neutron powder diffraction to establish the parameters of the oxygen sublattice and then single-crystal X-ray diffraction data for the final refinement. The structure is a cubic modification of the perovskite $ABO_3$ structure type. The refined composition is $Ba_{0.167}La_{0.548}Sr_{1.118}Ru_{0.377}Al_{0.290}O_{3.480}$, and with respect to the basic perovskite structure type it might be written as $(Ba_8La_{13.68}Sr_{34.32})(Al_{13.92}La_{12.64}Ru_{18.08}Sr_{19.36})$-$O_{192-x}$, with $x = 24.96$. The metal atoms lie on special positions. The *A*-type sites are occupied by Ba, La and Sr. The Ba atoms are located in a regular cuboctahedral environment, whereas the La and Sr atoms share the same positions with an irregular coordination of O atoms. The *B*-type sites are divided between two different Wyckoff positions occupied by Ru/Al and La/Sr. Only Al and Ru occupy sites close to the ideal perovskite positions, while La and Sr move away from these positions toward the (111) planes with high Al content. The structure contains isolated $RuO_6$ octahedra, which form tetrahedral substructural units.

## Comment

The crystal chemistry of ruthenium oxides is quite rich. Perovskite (Bouchard & Weiher, 1972; Shepard *et al.*, 1997), belonging to both cubic and hexagonal types, Ruddlesden–Popper (Cava *et al.*, 1995; Maeno *et al.*, 1994) and pyrochlore structure types (Bouchard & Gillson, 1971; Kobayashi *et al.*, 1995; Zhu *et al.*, 1997) are found in this family. The characteristic common to all of them is the presence of $RuO_6$ octahedra that form networks extending in one, two or three dimensions by corner- or edge-sharing. Additionally, compounds with isolated units of one, two or three octahedra have also been reported (Ebbinghaus, 2004; Darriet & Subramanian, 1995). This differing dimensionality, along with the fact that most of these compounds are metallic conductors, confer on them special interest as a medium for studying unusual physical properties. A good example is the compound $Sr_2RuO_4$ (Maeno *et al.*, 1994), which is the first layered perovskite-related compound that shows superconductivity without the presence of copper. Moreover, this species has been found to belong to the rare group of compounds showing spin-triplet superconductivity (Ishida *et al.*, 1998). Finally, hybrid ruthenocuprate materials show concomitant superconductivity and ferromagnetism, which is one of the most intriguing combinations of physical properties in modern solid-state chemistry and physics.

The crystal structure of the title compound reported here is part of a broad study concerning the synthesis and crystal chemistry of ruthenates. These compounds adopt complex crystal structures and disorder is normal. La and Sr usually occupy the same crystallographic positions, and their different oxidation states (+3 and +2 for La and Sr, respectively) are accommodated by distortion of the anion sublattice. The O atoms are thus forced to move away from their ideal positions and, furthermore, they might show partial occupancies in order to maintain charge neutrality. In this context, careful crystal structure determinations are hindered by the co-existence of oxygen, a light atom, with much heavier atoms such as Ru, Ba, La or Sr. To overcome this problem, in this work, the structure refinement was conducted using single-crystal X-ray and neutron powder diffraction data separately. The X-ray data provided basic information about the cationic substructure, while neutron powder diffraction data, because of the more substantial scattering length of oxygen for neutrons relative to those of the cations, was used to derive the relevant parameters of the oxygen substructure. Details of the two-part refinement are given in the *Experimental* section, and the final plot for the refinement from the neutron powder diffraction data is shown in Fig. 1.

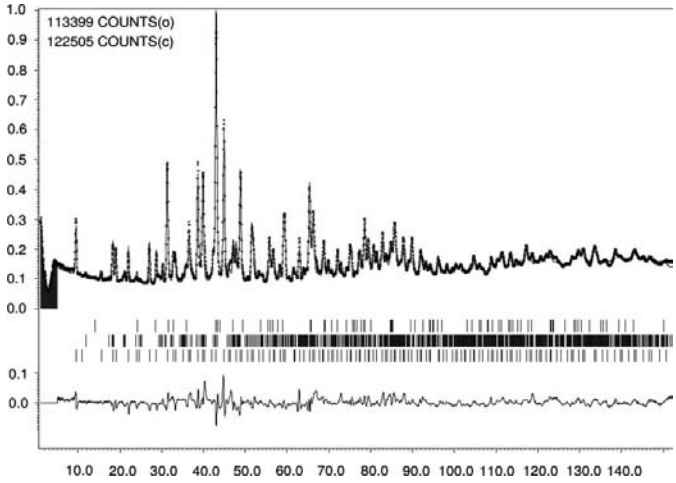


**Figure 1**
Rietveld refinement plot with neutron diffraction data.

  doi:10.1107/S0108270110013879 

The cationic formula (stoichiometric fraction of each element, considering only the cations) derived from the refined structural model, $Al_{0.12}Ba_{0.07}La_{0.22}Ru_{0.15}Sr_{0.45}$, agrees with the value obtained from microprobe analysis. Note that the percentages of the Ba and La cations must be compared with the sum obtained by energy-dispersive X-ray analysis. The composition derived from the refined model in wt% is $Ba_{7.7}La_{25.5}Sr_{32.8}(Al_{2.6}Ru_{12.7})O_{18.7}$.

The crystal structure of the title compound can be derived from the cubic perovskite $ABO_3$, where the *A* and *B* sites are occupied by the mixtures (Ba, La, Sr) and (Ru, Al, La, Sr), respectively. The distribution of the cations leads to a face-centred cubic superstructure with strongly distorted *B*-type cavities when these are occupied by Al, La or Sr. Projections of the structure down [100] and $[\bar{2}1\bar{1}]$, together with the undistorted perovskite arrangement, are presented in Fig. 2.

The *TRANSTRU* tool of the Bilbao Crystallographic Server was used to generate the coordinates of the ideal perovskite comparable with those of the present structure (Aroyo, Perez-Mato *et al.*, 2006; Aroyo, Kirov *et al.*, 2006). This program transforms a high-symmetry parent structure to a low-symmetry space group basis, splitting all possible Wyckoff positions. In our case, the parent phase is the $Pm\bar{3}m$ structure of $CaTiO_4$ and the low-symmetry space group is defined by the present space group $F23$ with a cell parameter four times that of perovskite. Comparing the structure so generated with the present one, it turns out that two of the split Wyckoff positions corresponding to *A*-type sites are vacant in the present structure. Using the compositional formula derived from the refined structural model, the cationic distribution in the ideal perovskite superstructure corresponds to the formula $(Ba_8La_{13.68}Sr_{34.32})(Al_{13.92}La_{12.64}Ru_{18.08}Sr_{19.36})O_{192-x}$, with $x = 24.96$.

Only Ba (Ba1 and Ba2 in *A* sites) and most (88.9%) of the Ru (Ru1 in *B* sites) present well defined oxygen coordination polyhedra (Fig. 3). Atoms Ba1 and Ba2 lie at the centres of regular cuboctahedra formed by 12 O atoms, and Ru1 is at the

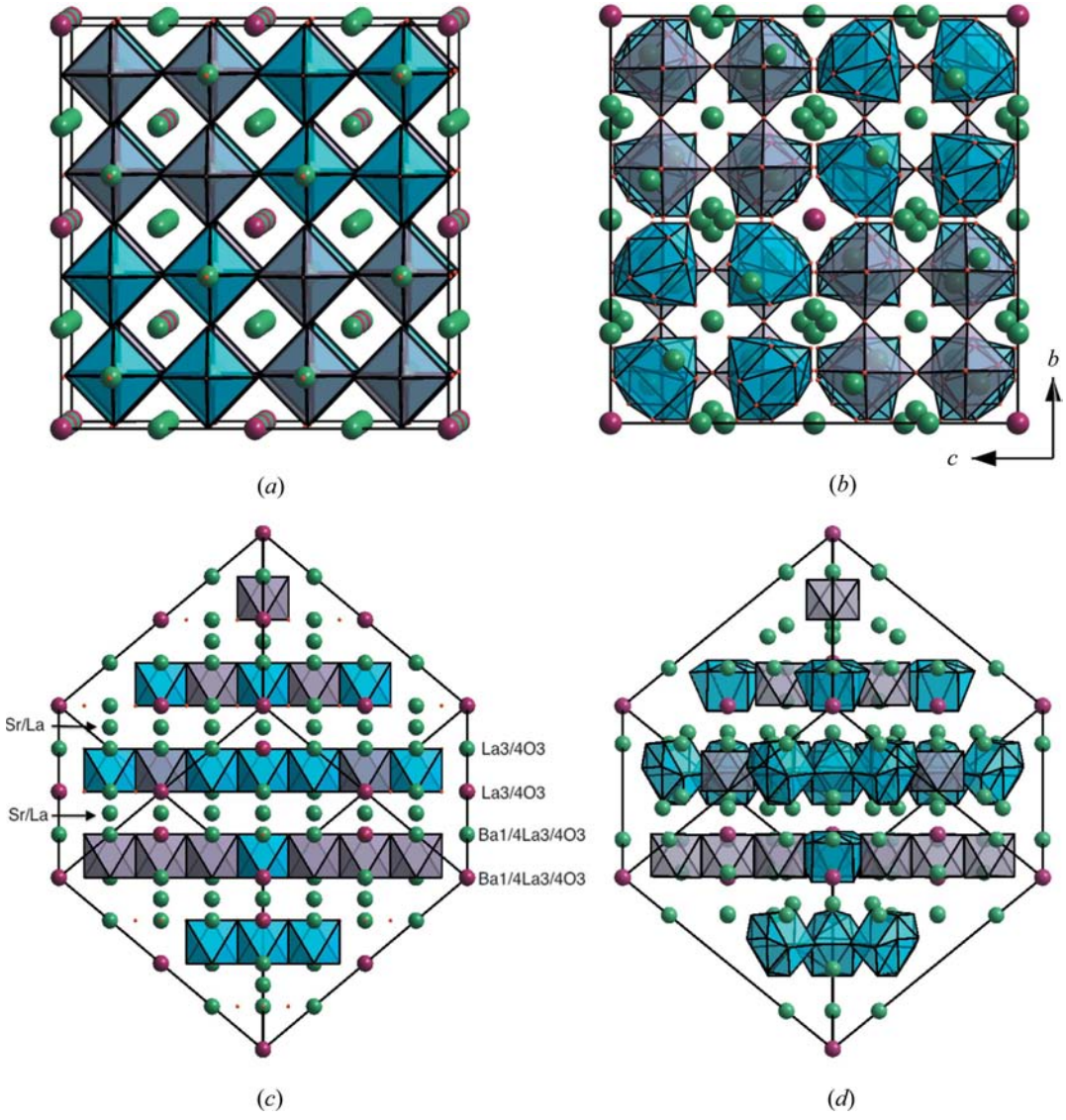


**Figure 2**
(*a*) and (*c*) show projections of the ideal perovskite, while (*b*) and (*d*) show projections of the title structure. Viewing directions: along [100] in (*a*) and (*b*), and along $[\bar{2}1\bar{1}]$ in (*c*) and (*d*). The labels in (*c*) indicate the compositions of the $AO_3$ and *B* layers.

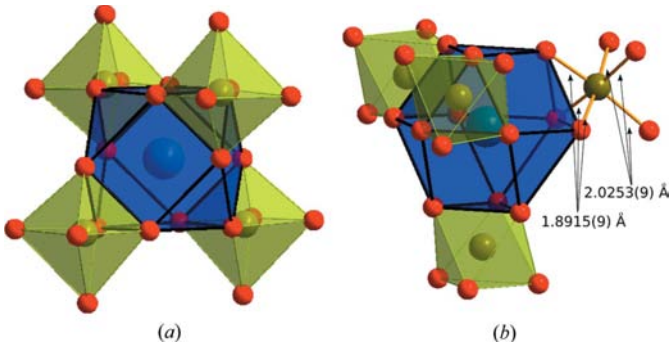


**Figure 3**
Substructural units formed from four $RuO_6$ octahedra enclosing the cuboctahedral cavity around (*a*) Ba1 and (*b*) Ba2.

centre of a slightly distorted octahedron. The Ba—O and Ru1—O distances (Table 1) are in agreement with values reported in the literature (Dusarrat *et al.*, 1996). It is worth noting that the O atoms involved in these coordination shells (O1 and O2) fully occupy their positions. These two cations and their coordination polyhedra form a characteristic structural unit, shown in Fig. 3. The cuboctahedra around Ba share four (out of eight) of the triangular faces with four Ru1-centred octahedra arranged as symmetrically as possible. The arrangement of this structural unit defines a face-centred cubic substructure. The remaining *A*- and *B*-type positions are occupied by (La1/Sr1, La3/Sr3) and (Al1/Ru2, La2/Sr2, La4/Sr4), respectively. The average coordination around these cations (Fig. 4) is rather irregular and further complicated by the fact that some of the coordinating O atoms (O3, O4, O5 and O6) have partial occupancy. The La/Sr—O distances and polyhedron shapes vary among these sites. The average coordinations at all of these sites are depicted in Figs. 4(*a*)–(*d*). The La1/Sr1 site has a major Sr component (64.3%), with an average environment of 12 O atoms at distances shown in Table 1. However, only nine bonds are possible. Besides six bonds to atoms O1 and O2, other combinations involving one congener of atom O3 and either two of O4 or two of O5 are possible. The La2/Sr2 sites are almost equally occupied by La/Sr, with an average environment of 15 O-atom sites. Only nine bonds actually exist (three O4···O6 and three O5···O6 vectors are too short for simultaneous occupation). At the La3/Sr3 site, the Sr occupancy is major (78.9%) and incompatible occupancy arises between O4···O6 and O5···O6. Two polyhedra, involving congeners of O1, O2 and of either (O4+O5) or O6, are possible. At the La4/Sr4 site, the presence of La is half that of Sr; this site exhibits the clearest coordination polyhedra. The average environment has nine O atoms but only six bonds may co-exist.

Atoms Ru2 and Al1 share the same crystallographic position. In the 12-coordinated polyhedron shown in Fig. 4(*e*), only two environments are possible. One is defined by atoms O3 and O6, which most probably occurs when the site is occupied by Ru. These O atoms define a strongly distorted octahedron with short but almost equal Ru2—O3 and Ru2—O6 distances. This seeming anomaly in the apparent distances could be explained, on the one hand, as a possible consequence of the inaccuracy of the Rietveld method used to determine the

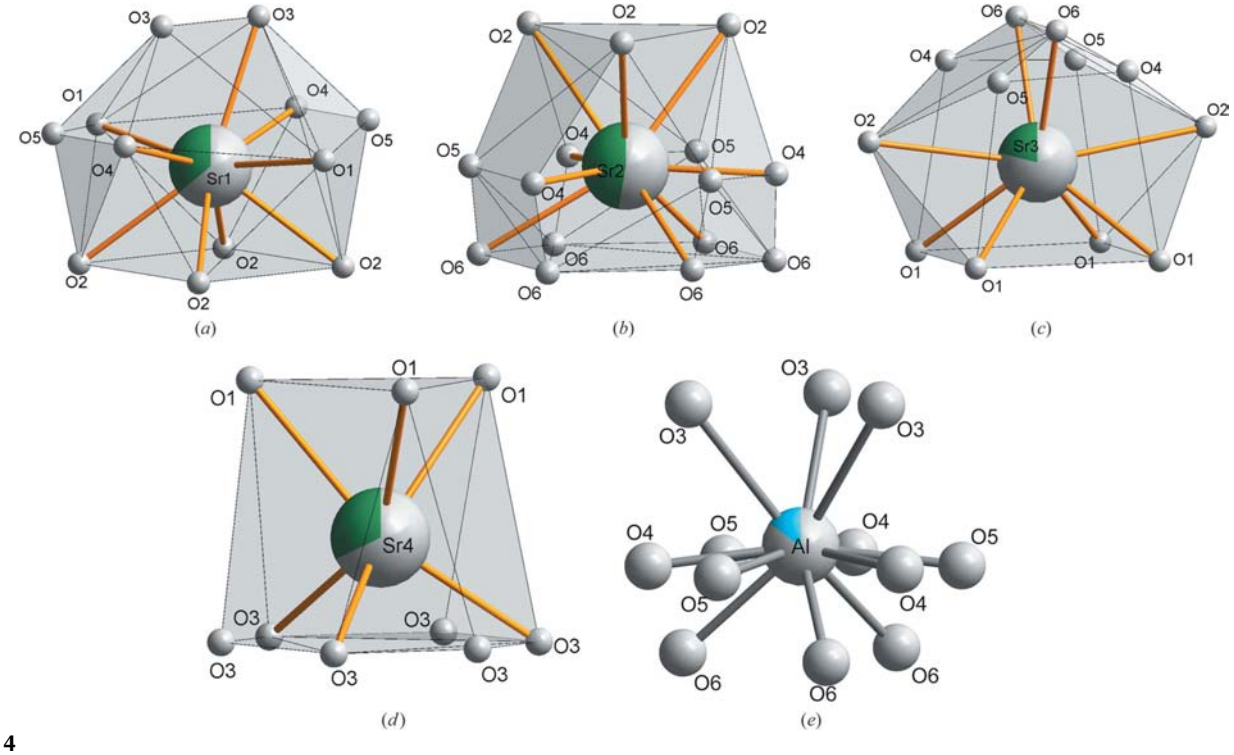


**Figure 4**
Average coordination polyhedra around (*a*) La1/Sr1, (*b*) La2/Sr2, (*c*) La3/Sr3, (*d*) La4/Sr4 and (*e*) Al1/Ru2. For clarity, generic atom labels without symmetry codes have been used for atoms in symmetry-related positions. In the electronic version of the journal, mixed colouring in the central atom represents the occupation fraction of La (green, darker)/Sr and Ru (blue, darker)/Al.

positions and site-occupation factors of the O atoms, and on the other hand as a result of the presence of O4 and O5 average sites too close to O3 and O6. Another possible environment around Al1/Ru2 would consist of either three congeners of O4 or three of O5. The short distance between them excludes the simultaneous presence of both types of atoms. In both cases, a triangular environment around Al1/Ru2 is formed, with a distance of 0.77 Å from the Al1/Ru2 position to the average plane defined by the six O4 and O5 positions.

The experimental cation–oxygen bond lengths can be tested with results from bond-valence analysis (Brown, 1992). Using bond-valence parameters from Brown & Altermatt (1985) for Al, Ba, La and Sr, and from Dusarrat *et al.* (1996) for Ru, atomic valences of 1.95 (1), 2.33 (2) and 5.05 (6) are found for atoms Ba1, Ba2 and Ru1, respectively. The values for Ba1 and Ru1 are close to the expected valences of 2 and 5, but the high value for Ba2 indicates residual bond strain at this site. The bond-valence calculations for the other cationic sites require proper application of the fractional occupancies corresponding to the different cation–oxygen bonds. As an example, a calculation for La1 using bonds to O1 (×2), O2 (×4), O3 (×1) and O4 (×3) gives a bond valence of 3.04.

## Experimental

The title compound was obtained unintentionally while attempting to synthesize $La_{0.4}Sr_{1.6}Cu_{0.4}Ru_{0.6}O_{4-x}$ using $BaCl_2$ as mineralizer. Stoichiometric amounts of dried $La_2O_3$, $SrCO_3$, CuO and $RuO_2$ were ground in an agate mortar. The resulting powder (1 g) was thoroughly ground with $BaCl_2$ (0.8 g). The final mixture was heated in air in an alumina crucible. The temperature was increased from room temperature to 1523 K over 7 h and kept there for 36 h. The temperature was then decreased to 1173 K at a rate of 10 K $h^{-1}$. After 5 h annealing at this temperature, the furnace was switched off.

The product, examined by optical microscopy, shows an apparent single phase of octahedrally shaped single crystals. The chemical composition obtained by electron microprobe microanalysis on a single crystal corresponds to the cation proportions Al 12%, (Ba 13%, La 13%), Ru 14%, Sr 46%, with a 3% estimated error and an average value for the Ba/La composition. Since these analyses were carried out on single crystals, impurities in the bulk sample are not reflected in the results. However, the sample used for powder diffraction does not correspond to a single phase. Indexing the neutron powder diffraction pattern using lattice parameters from the single-crystal diffraction data reveals the presence of a few unindexed peaks. The low intensities of these lines make the identification of the unknown phase difficult. The presence of the starting materials used in the synthesis was ruled out. The best match for the unindexed lines corresponds to a mixture of $Ba_3SrRu_2O_9$ and $Sr_2RuO_4$. Proportions of 18 and 3%, respectively, of these compounds were determined during the final Rietveld analysis based on the neutron powder diffraction data.

For single-crystal X-ray diffraction, a crystal of octahedral shape was selected for measurement of a highly redundant data set. Neutron powder diffraction data were collected at the FRM2 (Forschungs–Neutronenquelle–Heinz Maier–Leibnitz) neutron source on the Spodi diffractometer. A vanadium sample container was used, filled with 4.5 g of the synthesized material.

### Results from X-ray diffraction

*Crystal data*

$Al_{14}Ba_8La_{26.3}Ru_{18}Sr_{53.7}O_{167}$
$M_r$ = 14333.52
Cubic, $F23$
$a$ = 16.197 (1) Å
$V$ = 4249.2 (5) Å$^3$
$Z$ = 1
Mo $K\alpha$ radiation
$\mu$ = 26.68 mm$^{-1}$
$T$ = 295 K
0.14 × 0.13 × 0.09 mm

*Data collection*

Kuma KM-4/Oxford Xcalibur goniometer with an Oxford Sapphire2 detector
Absorption correction: Gaussian [*CrysAlis RED* (Oxford Diffraction, 2007); numerical absorption correction based on Gaussian integration over a multifaceted crystal model]
$T_{min}$ = 0.102, $T_{max}$ = 0.181
31971 measured reflections
1294 independent reflections
1126 reflections with $I > 3\sigma(I)$
$R_{int}$ = 0.042

*Refinement*

$R[F^2 > 2\sigma(F^2)]$ = 0.043
$wR(F^2)$ = 0.090
$S$ = 1.51
1294 reflections
65 parameters
1 restraint
$\Delta\rho_{max}$ = 3.45 e Å$^{-3}$
$\Delta\rho_{min}$ = −4.05 e Å$^{-3}$
Absolute structure: Flack (1983), with 584 Friedel pairs
Flack parameter: 0.51 (3)

### Results from neutron powder diffraction

*Crystal data*

$Al_{14}Ba_8La_{26.3}Ru_{18}Sr_{53.7}O_{167}$
$M_r$ = 14333.15
Cubic, $F23$
$a$ = 16.197 (1) Å
$V$ = 4249.2 (5) Å$^3$
$Z$ = 1
Neutron radiation, λ = 1.548 Å
$\mu$ = 0.01 mm$^{-1}$
$T$ = 298 K
Cylinder, 35 × 7 mm

*Data collection*

Powder diffractometer
Specimen mounting: vanadium can
Data collection mode: transmission
Scan method: step
Absorption correction: for a cylinder mounted on the $\varphi$ axis
(*JANA2006*; Petříček *et al.*, 2006)
$T_{min}$ = 0.945, $T_{max}$ = 0.947
$2\theta_{min}$ = 6.0°, $2\theta_{max}$ = 151.9°, $2\theta_{step}$ = 0.05°

*Refinement*

$R_p$ = 0.054
$R_{wp}$ = 0.060
$R_{exp}$ = 0.035
$R_{Bragg}$ = 0.071
$\chi^2$ = 21.623
3019 data points
61 parameters
1 restraint

The first refinement was based on single-crystal X-ray diffraction data. Reconstructed reciprocal space sections show cubic face-centred symmetry, with extinction rules compatible with space groups $F23$, $Fm\bar{3}$, $F432$, $F\bar{4}3m$, $Fm\bar{3}m$ and $F4_132$. Direct methods succeeded only with $F23$ and $F\bar{4}3m$, leading in both cases to the same structural model. Refinement in the space group $F23$ permitted the determination of the main features of the cationic structure. The refinement was started with equal occupancies for the La/Sr atoms in the $A$ sites of the perovskite superstructure, and similarly for Ru/Al/La/Sr at the $B$ sites, and with only O1 and O2, which form the octahedra around the Ru atoms. To avoid unrealistic total occupation factors, *i.e.* >1, the sum of the occupancies at the $A$ and $B$ sites was kept equal to 1. Successive refinement cycles including variable La/Sr occupancies converged, and difference Fourier maps revealed the remaining O atoms. At this point, the $B$-type sites with Ru/Al and La/Sr were differentiated. These latter two types of cations have disordered

**Table 1**
Selected bond lengths (Å) from X-ray diffraction data.

| | | | |
|---|---|---|---|
| Ba1—O1 | 2.958 (9) | La2/Sr2—O2$^{iv}$ | 2.613 (11) |
| Ba2—O2 | 2.891 (8) | La2/Sr2—O4$^{v}$ | 2.22 (8) |
| Ru1—O1 | 1.948 (9) | La2/Sr2—O5$^{ii}$ | 2.28 (8) |
| Ru1—O2 | 1.980 (12) | La2/Sr2—O6$^{ii}$ | 2.58 (2) |
| Ru2/Al1—O3 | 1.89 (4) | La3/Sr3—O1 | 2.559 (9) |
| Ru2/Al1—O4 | 2.17 (8) | La3/Sr3—O2$^{vi}$ | 2.870 (8) |
| Ru2/Al1—O5 | 2.18 (8) | La3/Sr3—O4$^{i}$ | 2.27 (8) |
| Ru2/Al1—O6 | 1.88 (2) | La3/Sr3—O5 | 2.26 (8) |
| La1/Sr1—O1 | 2.795 (9) | La3/Sr3—O6$^{vii}$ | 2.45 (3) |
| La1/Sr1—O2$^{i}$ | 2.558 (8) | La4/Sr4—O1$^{ii}$ | 2.675 (9) |
| La1/Sr1—O3$^{ii}$ | 2.43 (3) | La4/Sr4—O3 | 2.47 (4) |
| La1/Sr1—O4$^{iii}$ | 2.68 (8) | La4/Sr4—O3$^{vi}$ | 2.47 (4) |
| La1/Sr1—O5$^{ii}$ | 2.61 (8) | | |

Symmetry codes: (i) $z+\frac{1}{2}, x-\frac{1}{2}, y$; (ii) $-x+1, -y, z$; (iii) $y+\frac{1}{2}, -z, -x+\frac{1}{2}$; (iv) $x, -y+\frac{1}{2}, -z+\frac{1}{2}$; (v) $-x+1, y, -z$; (vi) $z, -x+\frac{1}{2}, -y+\frac{1}{2}$; (vii) $-y+\frac{1}{2}, z, -x+\frac{1}{2}$.

coordination polyhedra, and attempts to refine the occupancies of their O atoms with X-ray data failed. To overcome this problem, the neutron powder diffraction data were included in a refinement in which all minimized functions for the data blocks were combined with no additional weighting. In this analysis, two additional phases were included, *viz*. $Ba_3SrRu_2O_9$ (Zandbergen & IJdo, 1984) and $Sr_2RuO_4$ (Walz & Lichtenberg, 1993), to fit the experimental powder diffraction diagram, refining only their scale factors. A charge neutrality restriction was included over the atoms of the main phase. The occupancies and isotropic displacement parameters of the O atoms were refined successfully, but the occupancies of the La/Sr sites changed to values far from their proportions as measured in the compositional analysis. This probably occurs because these atoms have less contrast with neutrons than with X-ray scattering. The final refinement was performed using only the single-crystal X-ray data, fixing the occupational parameters of atoms O3, O4, O5 and O6 to the values obtained in the combined refinement and restricting the occupancies in accordance with an electroneutrality condition. All atoms were refined with anisotropic displacement parameters, except for atoms O3, O4, O5 and O6, which were refined with isotropic displacement parameters. High residual electron density at the Al1 site and a negative displacement parameter were corrected by replacing some Al content with Ru. In the final refinement, a refined Flack parameter (Flack, 1983) indicated an inversion twin. A final difference Fourier map shows the highest residual density values close to the Ba positions. Refinement in the space group $F\bar{4}3m$ also converges to similar *R* factors. Both structural models are similar, but atoms O4 and O5 in $F23$ merge into one atom in $F\bar{4}3m$. In $F\bar{4}3m$, the displacement parameter of this site becomes unusually large, which indicates that this atom represents an average of two different positions, corresponding to O4 and O5 in $F23$. This fact was used to select $F23$ instead of $F\bar{4}3m$. The final refinement plot for the neutron powder diffraction pattern is shown in Fig. 1. Residuals for the combined refinement are $R = 0.069$ and $wR = 0.073$ for the single-crystal data, and $R_p = 0.047$ and $wR_p = 0.062$ for the neutron powder diffraction data.

Data collection: *CrysAlis RED* (Oxford Diffraction, 2007) for X-ray data; Spodi instrument software, described by Hoelzel *et al.* (2007), for neutron powder data. Cell refinement: *CrysAlis RED* for X-ray data; *JANA2006* (Petříček *et al.*, 2006) for neutron powder data. Data reduction: *CrysAlis RED* for X-ray data; Spodi instrument software for neutron powder data. Program(s) used to solve structure: *SIR97* (Altomare *et al.*, 1999) for X-ray data; for neutron powder data, structure taken from X-ray data. For both refinements, program(s) used to refine structure: *JANA2006*; molecular graphics: *DIAMOND* (Brandenburg & Putz, 2005) and *CrystalMaker* (Palmer, 2009); software used to prepare material for publication: *JANA2006*.

This work was supported by the Deutsche Forschungsgemeinschaft (DFG) through grant No. SFB 484 and by the Basque Government (project No. IT-282-07). Technical support for the single-crystal measurements, provided by SGIker (UPV/EHU, MICINN, GV/EJ, ESF), is gratefully acknowledged.

Supplementary data for this paper are available from the IUCr electronic archives (Reference: FA3216). Services for accessing these data are described at the back of the journal.

## References

Altomare, A., Burla, M. C., Camalli, M., Cascarano, G. L., Giacovazzo, C., Guagliardi, A., Moliterni, A. G. G., Polidori, G. & Spagna, R. (1999). *J. Appl. Cryst.* **32**, 115–119.
Aroyo, M. I., Kirov, A., Capillas, C., Perez-Mato, J. M. & Wondratschek, H. (2006). *Acta Cryst.* A**62**, 115–128.
Aroyo, M. I., Perez-Mato, J. M., Capillas, C., Kroumova, C. E., Ivantchev, S., Madariaga, G., Kirov, A. & Wondratschek, H. (2006). *Z. Kristallogr.* **221**, 15–27.
Bouchard, R. J. & Gillson, J. L. (1971). *Mater. Res. Bull.* **6**, 669–679.
Bouchard, R. J. & Weiher, J. F. (1972). *J. Solid State Chem.* **4**, 80–86.
Brandenburg, K. & Putz, H. (2005). *DIAMOND*. Version 3. Crystal Impact GbR, Bonn, Germany.
Brown, I. D. (1992). *Acta Cryst.* B**48**, 553–572.
Brown, I. D. & Altermatt, D. (1985). *Acta Cryst.* B**41**, 244–247.
Cava, R. J., Zandbergen, H. W., Krajewski, J. J., Peck, W. F. Jr, Batlogg, B., Carter, S., Fleming, R. M., Zhou, O. & Rupp, L. W. Jr (1995). *J. Solid State Chem.* **116**, 141–145.
Darriet, J. & Subramanian, M. A. (1995). *J. Mater. Chem.* **5**, 543–552.
Dusarrat, C., Grasset, F., Bontchev, R. & Darriet, J. (1996). *J. Alloys Compd*, **233**, 15–22.
Ebbinghaus, S. G. (2004). *J. Solid State Chem.* **177**, 817–823.
Flack, H. D. (1983). *Acta Cryst.* A**39**, 876–881.
Hoelzel, M., Senyshyn, A., Gilles, R., Boysen, H. & Fuess, H. (2007). *Neutron News*, **18**(4), 23–26.
Ishida, K., Mukuda, H., Kitaoka, Y., Asayama, K., Mao, Z. Q., Mori, Y. & Maeno, Y. (1998). *Nature (London)*, **396**, 658–660.
Kobayashi, H., Kanno, R., Kawamoto, Y., Kamiyama, T., Izumi, F. & Sleight, A. W. (1995). *J. Solid State Chem.* **114**, 15–23.
Maeno, Y., Hashimoto, H., Yoshida, K., Nishizaki, S., Fujita, T., Bednorz, J. G. & Lichtenberg, F. (1994). *Nature (London)*, **372**, 532–534.
Oxford Diffraction (2007). *CrysAlis CCD* and *CrysAlis RED*. Oxford Diffraction Ltd, Abingdon, Oxfordshire, England.
Palmer, D. (2009). *CrystalMaker*. CrystalMaker Software Ltd, Yarnton, Oxfordshire, England.
Petříček, V., Dušek, M. & Palatinus, L. (2006). *JANA2006*. Institute of Physics, Czech Academy of Sciences, Prague, Czech Republic.
Shepard, M., McCall, S., Cao, G. & Crow, J. E. (1997). *J. Appl. Phys.* **81**, 4978–4980.
Walz, L. & Lichtenberg, F. (1993). *Acta Cryst.* C**49**, 1268–1270.
Zandbergen, H. W. & IJdo, D. J. W. (1984). *Acta Cryst.* C**40**, 919–922.
Zhu, W. J., Ting, S. T. & Hor, P. H. (1997). *J. Solid State Chem.* **129**, 308–311.